Miscible Blends of Two Crystalline Polymers. 3. Liquid−Liquid Phase Separation in Blends of Poly(vinylidene fluoride)/ Poly(butylene adipate)

Kenichi Fujita† and Thein Kyu*

Institute of Polymer Engineering, The University of Akron, Akron, Ohio 44325-0301

R. St. John Manley

Department of Chemistry, McGill University, Montreal, Quebec H3A 2A7, Canada

Received May 22, 1995; Revised Manuscript Received October 6, 1995⊗

ABSTRACT: Phase behavior and dynamics of liquid−liquid phase separation in binary blends of crystalline polymers, viz., poly(vinylidene fluoride) (PVF_2) and poly(butylene adipate) (PBA), have been studied by means of time-resolved light scattering. According to our previous calorimetric study, a single glass transition and two distinct melting endotherms were discerned over the entire composition range. The systematic movement of the glass transition with composition and the lowering of the melting point of the PVF_2 crystals indicate trends of a typical miscible blend. However, the dual melting peaks suggest that cocrystallization does not occur. In the melt state (∼60 deg above the melting temperature of the PVF_2 crystals), a thermally reversible lower critical solution temperature (LCST) was observed. Several temperature jump experiments were undertaken in a light-scattering apparatus at a 50/50 PVF_2/PBA composition from a single-phase melt state (200 °C) to a two-phase region (238, 240, 245, and 250 °C). A similar experiment was performed from a crystalline solid state (ambient temperature) to 238 and 240 °C for the elucidation of the effect of crystal melting on the kinetics of phase separation. Time evolution of structure factors (scattering intensity profiles) has been analyzed in the context of nonlinear and scaling theories of spinodal decomposition.

Introduction

The field of polymer−polymer phase separation has shown remarkable progress in the areas of thermodynamic phase equilibria and kinetics of phase decomposition.[1,2] This progress has been made primarily on amorphous−amorphous polymer blends.[3−7] There are very few studies on dynamic aspects of phase decomposition in amorphous−crystalline polymer blends,[8,9] and the number is even less for crystalline−crystalline polymer blends due to the involvement of complex crystalline morphology and the crystallization habit of the constituent polymers.[10] Moreover, the possibility of interference between crystallization kinetics and phase separation dynamics presents additional difficulty in the analysis, but it is extremely important for the understanding of the relationship between the resulting phase morphology and properties of the materials.

In an earlier paper,[11] we have reported the miscibility and crystallization behavior of a blend of PVF_2/poly(butylene adipate) (PBA). The choice of this pair is based on the facts that PVF_2 has potential miscibility with a number of ester-containing polymers including PBA and that both components are crystalline polymers. We have shown that a LCST phase diagram exists in the melt state well above the T_m of PVF_2 crystals. The lack of mutual interference between the crystal melting and liquid−liquid phase separation of the PVF_2/PBA blends makes the crystallization study in binary systems attractive, since crystallization kinetics can be studied in a variety of ways.[11] For instance, morphology development and kinetics of crystallization can be carried out by thermally quenching various blends from a single phase (melt state) into the temperature gap below the crystallization temperature (T_c) of PVF_2 but above the melting temperature (T_m) of PBA crystals or below their T_c's. Alternatively, thermal quenching may be performed from a two-phase region (above the LCST) to various crystallization temperatures to elucidate the effect of pattern formation on crystallization and the resulting morphology of the blends. Hence, in depth understanding of the liquid−liquid phase separation behavior is of crucial importance for the above crystallization studies. In this paper, we have investigated phase equilibria and dynamics of phase separation by employing time-resolved light scattering. The results of the time evolution of the structure factor are analyzed in the framework of nonlinear and dynamical scaling theories.

Experimental Section

PVF_2 (M_w = 140 000) and PBA (M_w = 14 000) were purchased from Polyscience, Inc. and Scientific Polymer Products, respectively. The as-received PBA was dissolved in dimethylformamide (DMF) and subsequently precipitated in methanol. PVF_2 was used as received without further purification. PBA and PVF_2 were dissolved in a common solvent (DMF) in various proportions. The polymer concentration was 5 wt %. The blend films were then solvent cast in a Petri dish at 50 °C and dried in a vacuum oven for 24 h at 70 °C. The cast films were stored in a desiccator at ambient temperature prior to use.[11]

Time-resolved light scattering used in this study is basically a static light-scattering apparatus which permits the simultaneous acquisition of the angular dependence of scattered intensity in one dimension (1-D) as a function of phase separation time. The apparatus consists of a low-power He−Ne laser light source (2 mW) with a wavelength of 632.8 nm. A 1-D Reticon detector (EG & G, Princeton Applied Research Co.) was used in conjunction with an Optical Multichannel Analyzer (OMA III, EG & G, Princeton Applied Research) to monitor the angular dependence of the scattered intensity in one dimension. The resolution of the silicon-diode array was

* To whom correspondence should be addressed.
† Present address: Department of Textiles and Clothing, Hiroshima Women's University, Minami-ku 734, Hiroshima, Japan.
⊗ Abstract published in *Advance ACS Abstracts,* November 15, 1995.

0024-9297/96/2229-0091$12.00/0

1024 pixels per 25 mm. One scan takes 60 ms. A couple of sample hot stages (sample holders with attached heating elements) were utilized in a side-by-side position for temperature (T) jump experiments; one was used for preheating and the other was set at the predetermined experimental temperatures. The specimen is rapidly transferred from one hot stage to the other within a fraction of a second. The temperature drops initially for 1−2 deg, and then it equilibrates within a few tens of seconds, typically depending on the temperature gap; e.g., the T jump from ambient to 240 °C took about 10 s. However, the T jumps from 200 to 240 °C require only about 2−3 s to equilibrate the sample.

The cloud point temperatures of various PVF_2/PBA compositions were determined by means of a light-scattering technique. The thickness of the blend film specimen for light-scattering studies was about 10 μm. Several T jump experiments were performed in situ under the light-scattering apparatus by transferring a 50/50 PVF_2/PBA blend rapidly from a crystalline state (ambient temperature) as well as from a single phase in the melt state (200 °C) to a two-phase region (238, 240, 245, and 250 °C). The evolution of scattering profiles was monitored by a Reticon camera as a function of elapsed time to mimic the kinetics of phase separation.

Results and Discussion

Phase Behavior. In an earlier paper,[11] the miscibility in blends of PVF_2 and PBA has been analyzed in terms of the phase diagrams of the mixture. The blends of PVF_2 and PBA undergo multiple phase transitions including a glass transition and melting of the PBA and PVF_2 crystalline phases, respectively. It was shown that all PVF_2/PBA blends prepared by the solution-casting method exhibited a single glass transition temperature varying systematically with composition, indicating the presence of an intimately mixed amorphous state. However, the observation of two distinct melting points, i.e., at ∼60 °C for PBA and at ∼175 °C for PVF_2, indicates that the two polymers crystallize separately. It was found that the equilibrium melting point $T_m°$ of the PVF_2 component systematically decreases with PBA content. From this melting point depression, a value for the Flory−Huggins interaction parameter of $\chi = -0.19$ (i.e., at 175 °C) was calculated, which shows that the two polymers are thermodynamically miscible in the melt. On the other hand, the $T_m°$ of PBA shows little or no variation with composition. We hypothesized that this behavior arises from morphological rather than thermodynamic effects. The results could be explained by taking into account that PVF_2 is partially crystalline around the melting point of PBA.

Cloud point measurements were undertaken for various PVF_2/PBA blends by monitoring the abrupt change of scattered intensity at an arbitrary scattering wavenumber, q, defined as $q = (4\pi/\lambda)(\sin\theta)/2$ where λ and θ are the wavelength of incident light and a scattering angle measured in the medium, respectively. Although the scattered intensity was measured over a range of scattering angles, we used the intensity at $q = 3\ \mu m^{-1}$ in determining the cloud point temperature because the intensity change was most prominent. The scattering peak increases during heating, but it decays when the process was reversed upon cooling. The heating rate was varied in the range of 0.5, 1.0, 2.0, and 5.0 °C/min, and the observed cloud point temperatures were extrapolated to the zero heating rate to establish an equilibrium cloud point phase diagram.

Figure 1 shows the LCST cloud point phase diagram with a broad minimum around 50−70%. The cloud point phase diagram is compared with the co-existence curve calculated on the basis of the Flory−Huggins

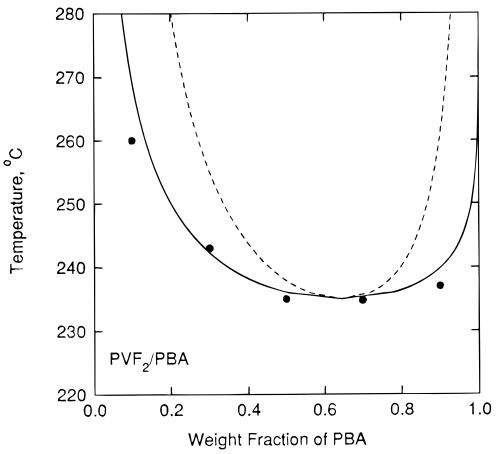

Figure 1. Temperature versus composition phase diagram of a blend of PVF_2/PBA calculated on the basis of the Flory−Huggins theory in comparison with the experimental cloud point phase diagram exhibiting a thermally reversible LCST. Note that the volume fraction of the blends was converted to weight fraction in the calculation by assuming the densities of PVF_2 and PBA to be 1.767 and 1.019 g/cm^3, respectively. The solid and dashed lines represent the calculated binodal and spinodal curves, respectively.

equation by assuming the statistical segment ratio (r_2/r_1) of the constituents to be 4.3/1, and the interaction parameter to be a simple function of inverse absolute temperature, i.e., $\chi = a + b/T$.[1] The a value was taken as 0.2 to account for the width of the LCST, and the b value was estimated directly from the critical temperature (T_c) and the critical composition of the LCST, viz., $\chi = a + (\chi_c - a)T_c/T$. In the calculation, the weight fractions were converted to volume fractions by assuming the densities of PVF_2 and PBA to be 1.767 and 1.019 g/cm^3, respectively. However, in the phase diagram (Figure 1), the calculated curves and the cloud points were replotted as a function of weight fraction in order to conform with the text. It is seen that the calculated binodal line accords well with the experimental cloud point plots; this proves useful as an aid in estimating the spinodal line to guide the experiment on dynamics of phase separation in the PVF_2/PBA blends. The critical point was found to be 0.62 at 235 °C. The cloud point curve implies that the PVF_2/PBA melts are completely homogeneous in the temperature region below the LCST but above the crystal melting temperature of PVF_2.

Kinetics of Phase Separation. In view of the large miscibility gap between the LCST and the crystal-melting temperature of PVF_2, it is interesting to compare the dynamics of phase separation between two temperature jump experiments, viz., (i) from a single-phase melt state (200 °C) to various two-phase temperatures and (ii) from a solid crystalline state (ambient temperature) to two-phase temperatures. Figure 2 illustrates the time evolution of scattering profiles from a single-phase (200 °C) to a two-phase region (238−250 °C). A scattering maximum first appears in the vicinity of $q_m \sim 6-7\ \mu m^{-1}$ and shifts rapidly to a smaller wavenumber as a result of phase growth. In the reverse quench experiment, the 50/50 blend was first equilibrated at 200 °C for 5 min in the single phase. The specimen was transferred rapidly to a hot stage controlled isothermally at 240 °C and was allowed to phase separate for 2 min; then the sample was quenched rapidly to a single phase (200 °C). Figure 3 exhibits a rapid time decay of the scattering intensity following a T quench from 240 to 200 °C, indicating that phase

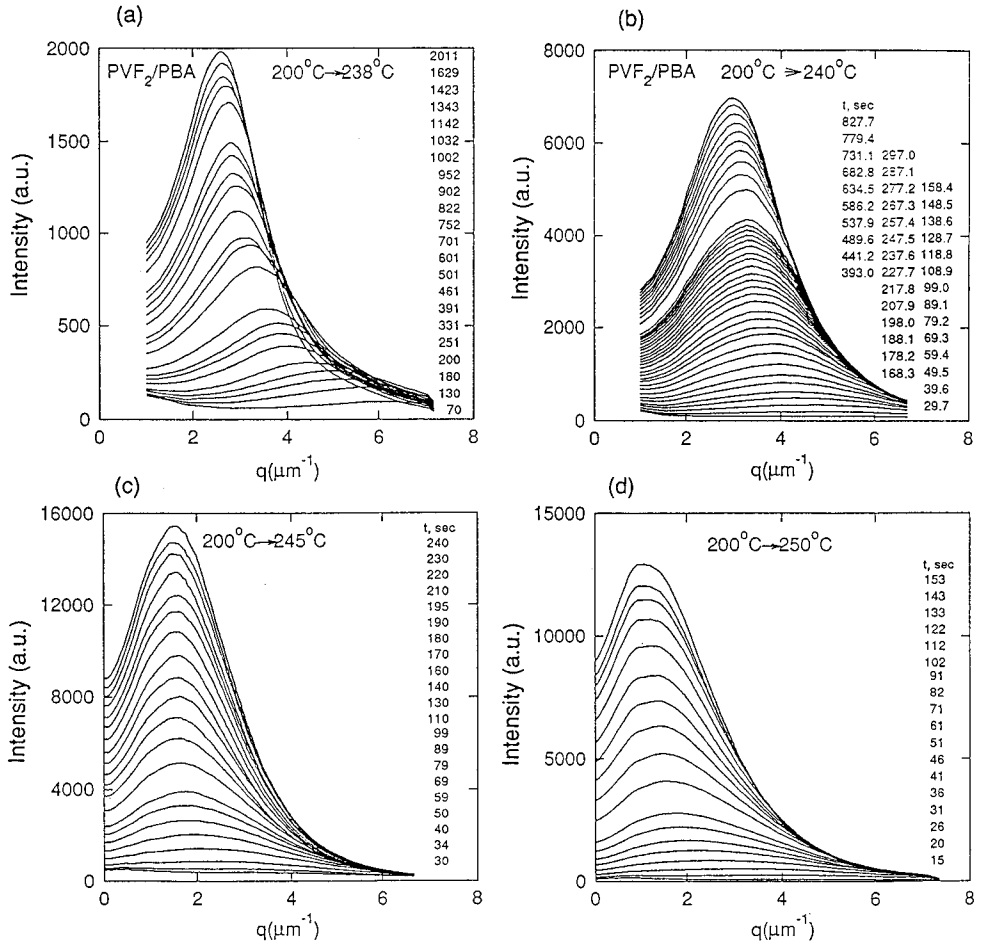

Figure 2. Time evolution of scattering profiles of the 50/50 PVF_2/PBA composition after following various temperature jumps from a single phase in the melt (200 °C) to two-phase temperatures (a) 238, (b) 240, (c) 245, and (d) 250 °C.

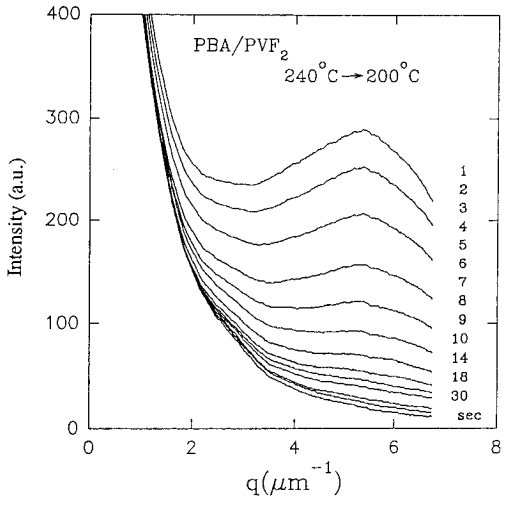

Figure 3. Time decay of scattering curves of the 50/50 PVF_2/PBA blend following a reverse *T* quench from a two-phase (240 °C) to a single-phase melt state (200 °C) exhibiting a homogenization process (phase dissolution).

dissolution is seemingly completed within 30 s. The rapid homogenization makes analysis of the dynamics of phase dissolution impractical and thus was not pursued further. Nevertheless, we are able to confirm that the observed LCST is thermally reversible, which is the prerequisite for a true LCST. In the phase separation process, there is no discernible period that can be characterized as an early stage of phase separation, as predicted by the linearized Cahn−Hilliard theory;[12] therefore we focus on the late stages of spinodal decomposition (SD).

A common rule that governs a nonequilibrium dynamical evolution toward thermodynamic equilibrium is a scaling law which suggests the similarity of a structure factor $S(q,t)$ at later times to that of earlier times. Here, the structural growth involves a change in length scale only while preserving the statistically similar structure, often known as a "self-similar structure". This kind of dynamical evolution is nonlinear in character and customarily analyzed in the context of a power law scheme;

$$q_m(t) = \Lambda(t)^{-1} \sim t^{-\alpha} \tag{1}$$

and

$$I_m(t) = \langle \eta(t)^2 \rangle \Lambda(t)^3 \sim t^{\beta} \tag{2}$$

where the subscript m stands for the maximum value. $\langle \eta(t)^2 \rangle$ and $\Lambda(t)^3$ represent the mean-square fluctuation of refractive indices and the length scale of the domains, respectively. The exponents, α and β, have been predicted by various theories.[12] The notable values for the late stages of SD are $\alpha = 1/3$ and $\beta = 1$, which have been predicted by the classical evaporation−condensation model of Lifshift-Slyozov[12] and the cluster dynamics of SD by Binder and Stauffer with $\beta = 3\alpha$.[13] On the other hand, Siggia[14] obtained a similar relationship, but with $\alpha = 1/3$ for the intermediate state and $\alpha = 1$ for the late stage of SD where the instability due to hydrodynamic flow becomes dominant.

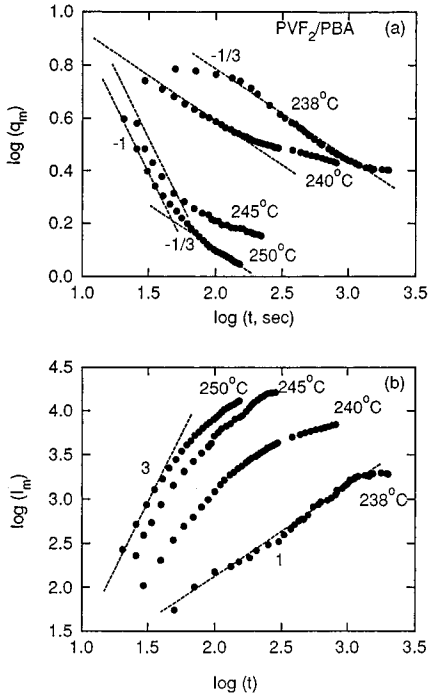

Figure 4. log−log plots of (a) $q_m \sim t^{-\alpha}$ and (b) $I_m \sim t^{\beta}$ following a T jump from 200 to 238, 240, 245, and 250 °C.

Parts a and b of Figure 4 show the log−log plots of the maximum wavenumber q_m and the corresponding scattered intensity maximum I_m versus phase separation time, respectively. The data at the T jump of 238 °C can be approximately represented by slopes of $-1/3$ and -1 in the log q_m vs log t and log I_m vs log t plots, respectively. These exponent values ($\alpha = 1/3, \beta = 1$, and $\beta = 3\alpha$) are in good accord with the dynamics of cluster coalescence, suggested by Binder and Stauffer[13] for the late stages of SD or by Siggia[14] for the intermediate stage. The predicted exponent of $1/3$ has been borne out experimentally in a number of amorphous polymer blends.[2−7] At 240 °C, the exponent α is approximately $1/3$ in the early times, but it crosses over to a smaller value as time elapses. The value of β is about 2, thus $\beta > 3\alpha$, implying a transition from intermediate to late stages of SD.

At higher T jumps to 245 and 250 °C, the coarsening process is seemingly expedited, leading to the larger initial slopes of approximately $\alpha = 1$ and $\beta = 3$. This growth process is consistent with the prediction of Siggia[14] for the late stages of SD where the hydrodynamic flow is dominant; such coarsening is known to be driven by surface tension. Later, a crossover of the slopes to a smaller value ($\alpha = 1/3$) takes place, suggesting that the growth process has slowed down due to the breakup of the bicontinuous phase associated with the physical pinning effect often observed in the off-critical quenching.[2,8] The T jump gap dependence of the growth exponent from $\alpha = 1/3$ to 1 has been observed for a number of polymer blends.[3−7] The present result is not surprising in view of the fact that the LCST is located well above the crystal-melting temperatures of the constituents; thus the system simply behaves like polymeric liquid mixtures and follows a classical liquid−liquid phase separation behavior.

The next question is what would happen if the T jump experiment is performed from the crystalline state to the two-phase region. In order to have a valid comparison, the 50/50 PVDF/PBA blend was melted once at 200 °C for 5 min to assure complete melting and subsequently air-quenched to room temperature. The blend was rapidly transferred to the hot stage controlled isothermally at 240 °C. Parts a and b of Figure 5 depict the time evolution of scattering curves following a T jump from room temperature (25 °C) to 240 °C. The scattered intensity diminishes as crystals first melt away and appears to be completed within 13.9 s (Figure 5a). After 99 s, a scattering maximum redevelops at a wider scattering angle when liquid−liquid phase separation takes place (Figure 5b). A similar T jump was conducted from ambient temperature to 238 °C.

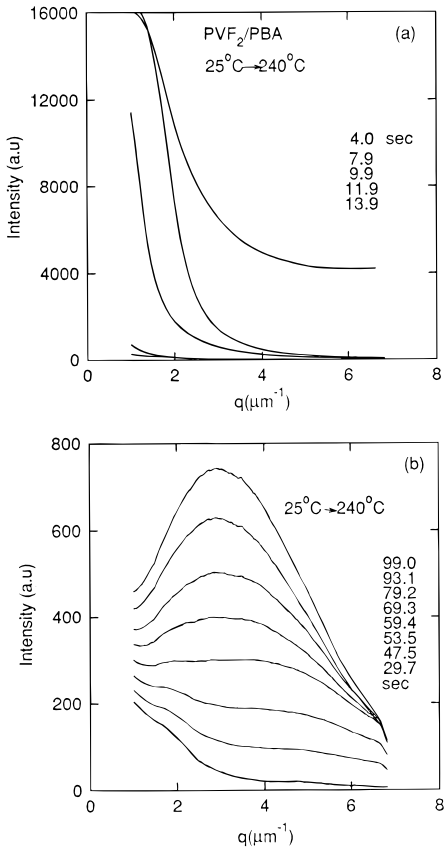

Figure 5. Time evolution of scattering profiles of the 50/50 PVF_2/PBA blend following a T jump from a solid crystal phase (ambient temperature) to a two-phase temperature of 238 °C.

As shown in Figure 6a, two distinctive features can be noted. First, the initial concentration fluctuation is large, as evidenced by the smaller q_m as compared to that obtained in the T jump from 200 to 238 °C. Second, the growth exponent α is close to $1/5$, which is somewhat smaller than the predicted $1/3$ value for a typical liquid−liquid phase separation, and $\beta = 1.33$ with $\beta > 3\alpha$. At a glance, the present observation is in line with the suggestion by Binder and Stauffer[13] that the droplet size increases according to $t^{1/3}$ in a liquid and $t^{1/6}$ in a solid phase. However, it seems highly unlikely that the solid-like materials would be still undergoing a melting transition at such an elevated temperature well above the T_m of the constituents, although such a possibility cannot be ruled out. Another possibility is due to the proximity of the T jump temperature of 238 °C to the spinodal temperature of the 50/50 composition (Figure 1), where the diffusivity could be zero or at least very small. When the crystalline structures such as spherulites melt, the initial concentration fluctuations in the system would be large. The molecular diffusion near the spinodal point may be so slow that there would not be sufficient time for completing the homogenization

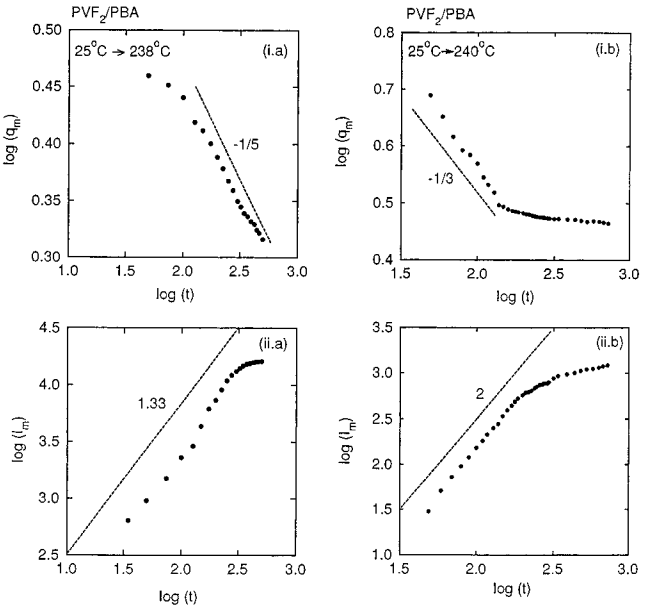

Figure 6. log−log plot of (i) $q_m \sim t^{-\alpha}$ and (ii) $I_m \sim t^{\beta}$ following a *T* jump from ambient temperature to (a) 238 °C and (b) 240 °C.

process. These residual large fluctuations probably serve as nuclei upon which growth occurs. This probably explains why the q_m of the *T* jump from ambient to 238 °C (Figure 6a) is smaller than that from the *T* jump from the single-phase temperature (200 °C) to 238 °C (Figure 4a). It should be pointed out that the final fluctuation sizes of the two *T* jumps are not appreciably different, whereas the initial fluctuation length scale of the *T* jump from the solid crystalline state to 238 °C is larger than that at 240 °C. Hence the growth exponent of the latter would be naturally smaller. It seemingly suggests that the initial large concentration fluctuations associated with the crystal melting and the slow molecular diffusion may be responsible for the smaller growth rate. At a deeper *T* jump of 240 °C, the diffusion becomes appreciably greater relative to that at 238 °C so that homogenization could be completed before phase separation occurs again. Hence, the system exhibits a normal liquid−liquid phase separation behavior with an initial slope of $\alpha = {}^1/_3$, but $\beta = 2$, thus $\beta > 3\alpha$ (Figure 6b). As phase separation advances further, the slope decreases due to the pinning effect which is a signature of an off-critical quenching.[2,8] At large *T* jumps, it appears that the starting state, whether it is crystalline or melt (single phase), does not exert significant influence on the growth behavior of liquid−liquid phase separation in the present 50/50 PVF_2/PBA blend.

Self-Similarity Tests. The growth of phase-separated domains involves a change in length scale (size) as well as in structure (shape). It is important to establish the fact that the length scale (size) is the only parameter that is involved in the phase growth without any change in the structure in a statistical sense. Such a structure is called a "self-similar structure". The self-similar behavior has been characterized customarily in terms of the dynamic scaling of Furukawa.[15] The time evolution of the structure factor or scattered intensity *I(q,t)* may be expressed for three-dimensional growth as

$$I(q,t) = \langle \eta(t)^2 \rangle \, \Lambda(t)^3 \, S(x) \qquad (3)$$

where $\langle \eta(t)^2 \rangle$ is the mean square fluctuation of refractive

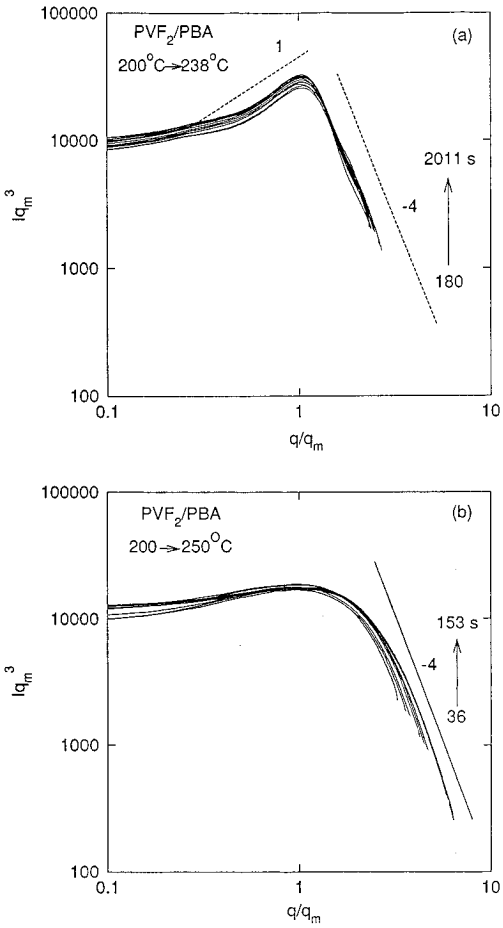

Figure 7. Change of $I(q)\ q_m^3$ versus q/q_m in double logarithmic plots of the 50/50 PVF_2/PBA blend at (a) 238 °C and (b) 250 °C. The slopes are shown for reference.

indices, *S(x)* is the scaled structure factor, and $x = q\xi(t)$. Here, $\xi(t)$ in turn relates to the wavelength of periodic structure $\Lambda(t)$, i.e., $\xi(t) = \Lambda(t)/2\pi = 1/q_m(t)$. By insertion of this equation into eq 3, the scaled structure factor may be rewritten as

$$S(x) \sim I(q,t)\ q_m^3(t) = F(x) \qquad (4)$$

In the late stages, the mean-square fluctuation, $\langle \eta(t)^2 \rangle$, reaches its limiting value $\langle \eta^2 \rangle$ as the interface boundary becomes sharp; thus *F(x)* should be scaled with a single length parameter $\xi(t)$. The temporal scaled structure factors can be superimposed reasonably well to form a single master curve (Figure 7). Although the resulting master curve is slightly broad, it is reasonable to conclude that the system is self-similar, implying that the domain structure in the early period of phase separation is similar in a statistical sense to that in the later times. In other words, the length scale is the only parameter that gets larger during phase separation without changing its shape.

Now, it is of interest to investigate the detailed study of *F(x)* at larger *x* regions, as it should provide additional information on the intricate local structure such as interface sharpness. It is worthwhile to explore this behavior by analyzing the shape of the structure factor *F(x)* which may be scaled by a single length parameter as[16]

$$F(x) = (1 + \gamma/2)x^2/(\gamma/2 + x^{2+\gamma}) \qquad (5)$$

where $\gamma = d + 1$ for an off-critical mixture and $\gamma = 2d$

for a critical mixture; d is the dimensionality. For three-dimensional growth, $F(x) \sim x^2$ for $x < 1$, and for $x > 1$, $F(x) \sim x^{-6}$ (for a critical mixture) and x^{-4} (for an off-critical mixture). Furukawa proposed later that $F(x) \sim x^4$ at $x < 1$, if the quench depth were large. The crossover from the slope of -6 to -4 at large wavenumbers has been observed in the critical mixture of some polymer blends. The scaling exponent in the small q limit is often difficult to determine due to parasitic scattering. As shown in Figure 7, the scaled structure factor exhibits a slope of ~ 1 at $x < 1$ which is appreciably smaller than the predicted value of 2 for shallow quenches and 4 for deep quenches. The incomplete removal of parasitic scattering and stray light arising from the beam stop may be responsible for this discrepancy. At $x > 1$, the slope of -4 was obtained as typical for an off-critical quenching. The observed slope of -4 is simply a manifestation of a sharp interface of the domain boundaries.

Conclusions

We observed that the blends of PVF_2/PBA revealed an LCST above their crystal-melting temperatures. The LCST is thermally reversible. Time-resolved scattering experiments following a T jump from a melt single phase to a two phase region showed that the domains grow according to $t^{1/3}$ law at shallow T jumps. At larger T jumps, the growth exponent changed according to the power law of t^1. The shallow T jump from a crystalline solid state to a two-phase temperature (238 °C) near the spinodal point showed some influence of the crystal melting on the liquid−liquid phase separation of the 50/50 PVF_2/PBA blend; i.e., the time evolution of the structure factor exhibited a larger initial concentration fluctuation and a smaller growth exponent of $^1/_5$ as compared to that of the T jump from the single-phase temperature (200 °C) to 238 °C. Although the suggestion of the presence of slowly melting solid-like materials in the melt is highly unlikely, such a possibility cannot be ruled out. If the T jump from the solid crystalline state is sufficiently deep into the immiscibility gap (higher T jumps), the homogenization process following the crystal melting can be completed in the short period. Hence, there is no appreciable difference in the growth behavior regardless of whether the T jump is started from the solid crystalline phase or a melt single phase to a final two phase region (>240 °C).

Acknowledgment. R.St.J.M. gratefully acknowledges support in the form of an operating grant from the Natural Sciences and Engineering Research Council of Canada. K.F. thanks Hiroshima Women's University, Province of Hiroshima, for support of his sabbatical leave at the University of Akron.

References and Notes

(1) Olabisi, O.; Robeson, L. M.; Shaw, M. T. *Polymer-Polymer Miscibility*; Academic Press: New York, 1979.
(2) Hashimoto, T. *Phase Transitions* **1988**, *12*, 47.
(3) Sato, T.; Han, C. C. *J. Chem. Phys.* **1986**, *88*, 2057.
(4) Hashimoto, T.; Kumaki, J. *Macromolecules* **1986**, *19*, 763.
(5) Bates, F. S.; Wiltzius, P. *J. Chem. Phys.* **1989**, *91*, 3285.
(6) Kyu, T.; Saldanha, J. M. *Macromolecules* **1988**, *21*, 1021.
(7) Kyu, T.; Lim, D. S. *Macromolecules* **1991**, *24*, 3645.
(8) Inaba, N.; Yamada, T.; Suzuki, S.; Hashimoto, T. *Macromolecules* **1988**, *21*, 407. Hashimoto, T., Takenaka, M., Izumitani, T. *J. Chem. Phys.* **1992**, *97*, 679.
(9) Tanaka, H.; Nishi, T. *Phys. Rev. A* **1989**, *39*, 783.
(10) Kyu, T.; Yang, J. C. *Macromolecules* **1990**, *23*, 176, 182.
(11) Penning, J. P.; St. J. Manley, R. *Polym. Prepr. (Am. Chem. Soc., Div. Polym. Chem.)* **1995**, *36*; *Macromolecules* **1996**, *29*, 77 and 84 and references therein.
(12) Gunton, J. D.; San Miguel, M.; Sahni, P. S. In *Phase Transitions and Critical Phenomena*; Domb, C., Lebowitz, J. L., Eds.; Academic: London, 1983; Vol. *8*, p 267.
(13) Binder, K.; Stauffer, D. *Phys. Rev. Lett.* **1974**, *33*, 1006.
(14) Siggia, E. D. *Phys. Rev. A* **1979**, *20*, 595.
(15) Furukawa, H. *Phys. Rev. Lett.* **1979**, *43*, 136.
(16) Furukawa, H. *Physica A* **1984**, *123*, 497.

MA950692P